LA-UR- 10-08161

Approved for public release; distribution is unlimited.

Title:	MCNP Simulations of Material Exposure Experiments (U)
Author(s):	Brian Temple
Intended for:	Report for MST Division

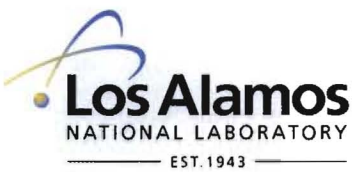

Form 836 (7/06)

MCNP Simulations of Material Exposure Experiments (U)

Brian Temple

Introduction

Simulations of proposed material exposure experiments were performed using MCNP6. The experiments will expose ampules containing different materials of interest with radiation to observe the chemical breakdown of the materials. Simulations were performed to map out dose in materials as a function of distance from the source, dose variation between materials, dose variation due to ampule orientation, and dose variation due to different source energy. The complete set of results are in the *gif_cave.xlsx* EXCEL file. This write up is an overview of the simulations and will provide guidance on how to use the data in the spreadsheet.

Descriptions of the experiments and the simulations

The experiments were and will be performed in lead caves constructed at Sandia. The radiation source is ^{137}Cs which emits 662 keV gammas. Additional experiments using an ^{241}Am 60 (59.5) keV gamma source are also under consideration. The materials of interest are contained in two sets of ampules that are 6 inches long and have slightly different diameters. The first set of ampules has a flange diameter of 2.75 inches and tube diameter of 1.505 inches. The second set of ampules has a flange diameter of 3.375 inches and tube diameter of 1.875 inches. Each set of ampules has side walls of thickness 0.1875 inches and end wall thicknesses of 0.2 inches.

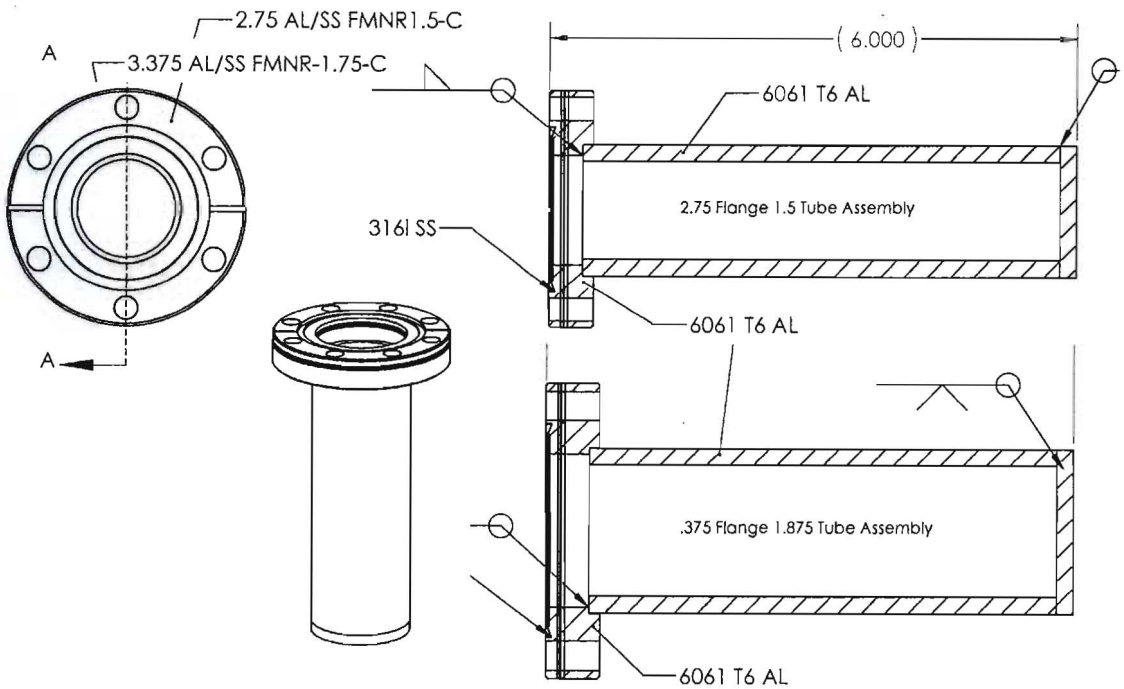

Figure 1. Drawings of the ampoules.

The ampoules were placed at different distances from the source to represent multiple years of exposure to materials of interest in a condensed amount of time. Simulations were made to spatially map out dose rates so that the correct accelerated exposure can be determined for each ampoule. The radial calculations were made for both sets of ampoules with the source placed in the middle of the cave and in a corner. The *gif_cave.xlsx* EXCEL file contains all of the simulation results.

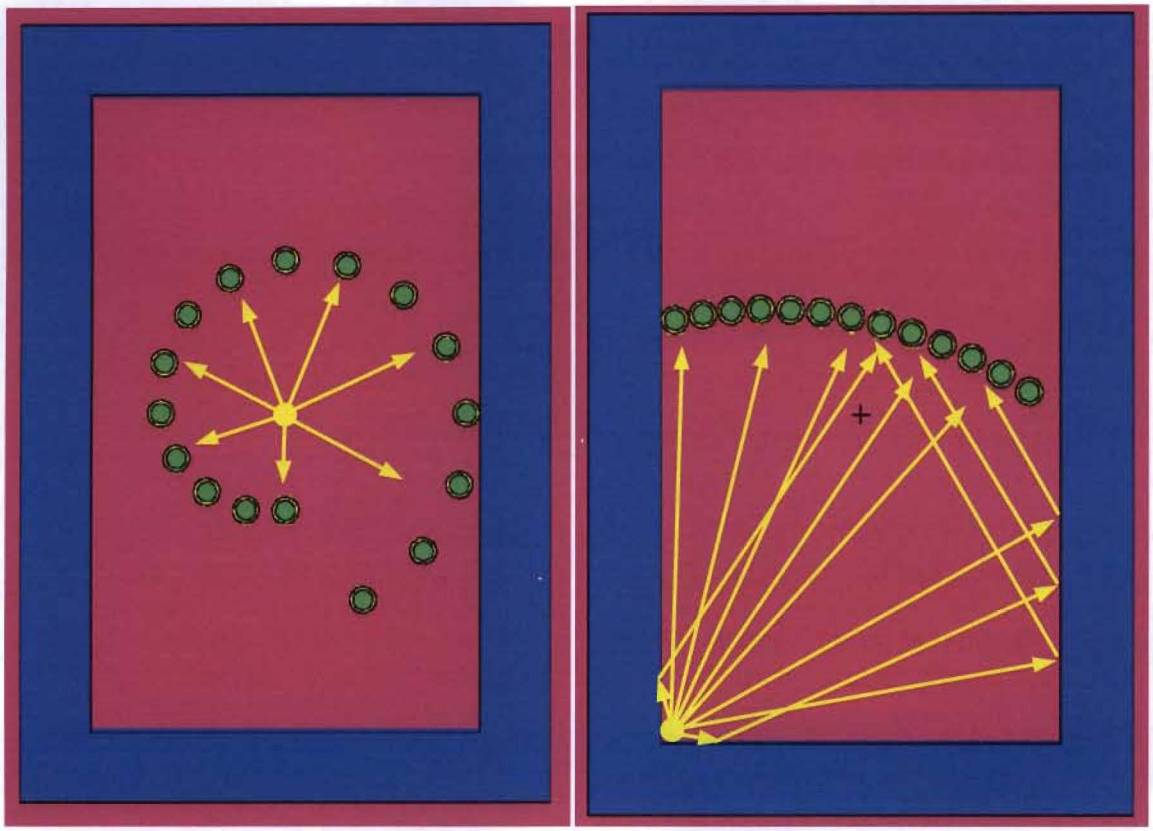

Figure 2. MCNP plots of the ampoules (green) in the lead cave (blue). The source is shown as a yellow circle and its emissions are arrows (yellow).

The lead cave is shown in blue. The ampoules are green and the source is represented as a yellow circle. The emission from the source is given as yellow arrows. The source in the corner will have more scatter from the cave walls and that scatter is illustrated with the multi-directional arrows. The ampoules were positioned with their centers ranging from 2 cm to 97cm in order to map out the range of distances possible in the cave. Any distance beyond 30 cm requires the source to be positioned in the corner. The material used as a baseline for the simulations is LK3626. The source strengths for the plots use the ^{137}Cs emission rates for a single cylinder, which is 147 milliCuries. Results per source particle exist in the spreadsheet and can be re-scaled for the dose at any source strength.

Separate simulations were made to address dose changes due to the orientation of the ampoules with respect to the source and having different materials in the ampoules. Simulations rotating the ampoules toward and away from the source were made with and without the heater coils around the ampoules to quantify the orientation effects.

Simulations with different materials in the ampoules were also made so the dose to the LK3626 at different distances can be adjusted for the different materials. These calculations were made so that predictions of the dose to the ampoules can be made for different positioning and distancing of the ampoules to the source in the caves.

Simulations results

The plots of the dose to the LK3626 in the ampoules are plotted in Figures 3 and 4. The dose rates for the center source and corner source are plotted separately in each figure, but appear to follow the same curve. The best fits to the data are power law equations which were fit to the different source plots separately and to all total dose data over the entire span of radii. The total curve fits over all radii should be sufficient for determining dose rate as a function of distance from the source, regardless of the source position. The dose rate curves have a similar shape that reflects the $\sim 1/r^2$ fall off of the dose. The exponential in the fit is not two since there are scatter effects in the cave. The total dose at the farthest positions from the source is nearly two orders of magnitude smaller than the total dose near the source. The scatter contribution to the dose (scatter dose) is more influenced by the position of the source rather than the size of the ampoule. The scatter contribution to the dose is nearly constant for the center source and is around 2 orders of magnitude smaller than the total dose. The scatter dose from the corner source changes with the ampoule distance from the source and is around an order of magnitude smaller that the total dose. The scatter dose at the farthest positions from the source becomes comparable to the scatter dose for the center source.

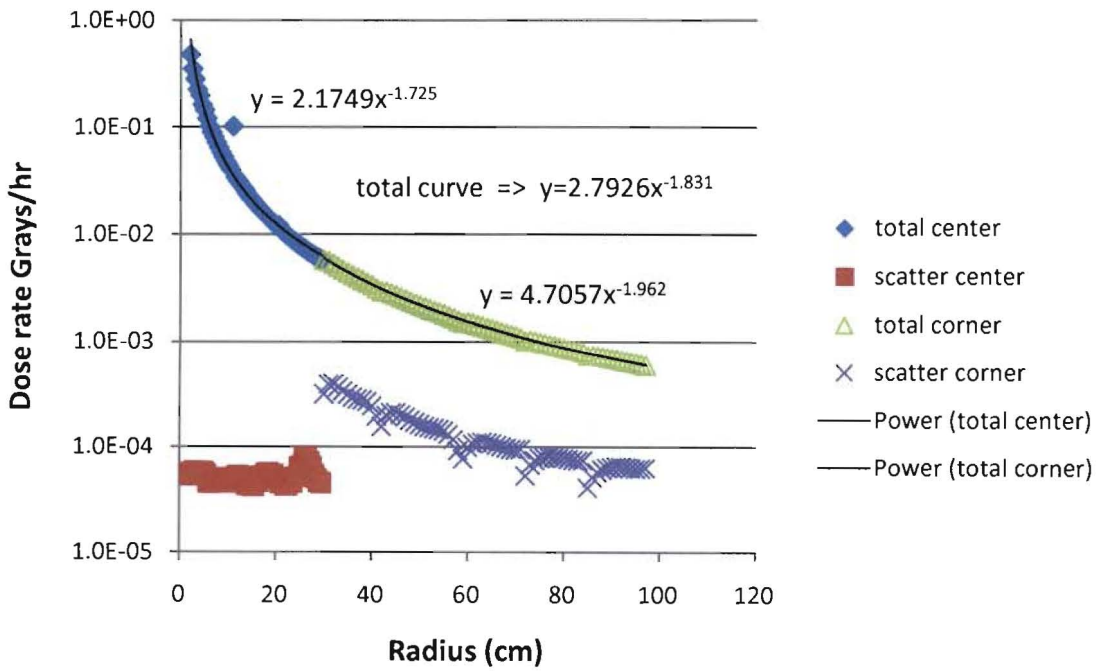

Figure 3. Dose rate curves for the 2.75in ampoules from a single source of ^{137}Cs.

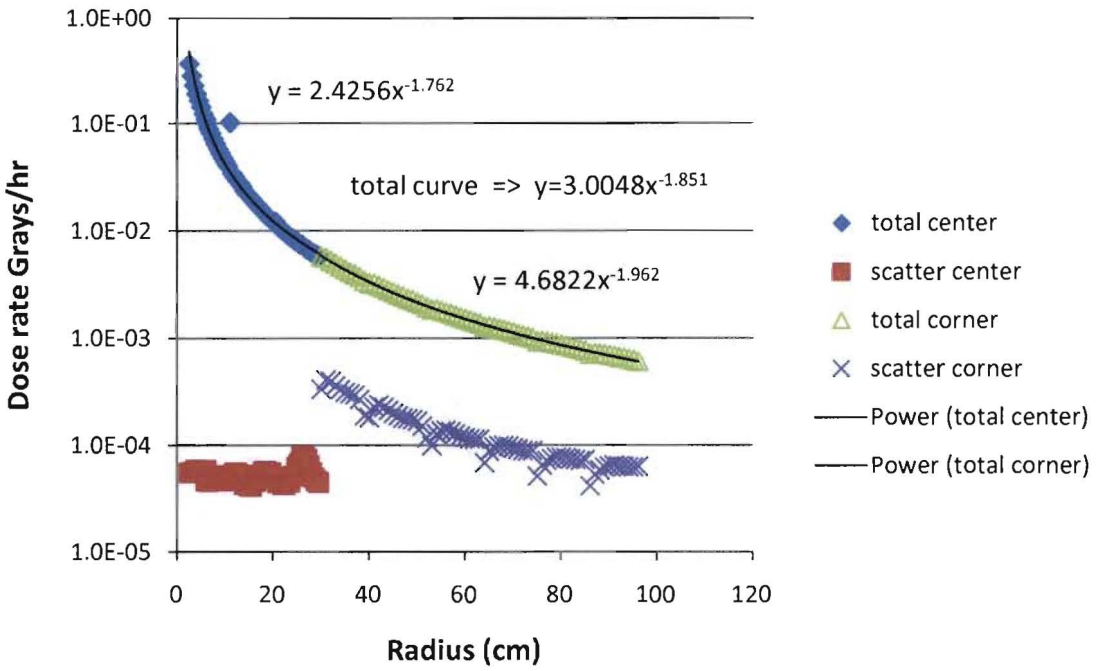

Figure 4. Dose rate curves for the 3.375in ampoules from a single source of ^{137}Cs.

The differences in dose rate due to the ampoule orientation with respect to the source are plotted in Figure 5. The source is in the center of the cave and the ampoules are rotated toward or away from the source at a distance of 15cm from the source. The results are labeled by their ampoule flange size and by the presence of a heating coil around the ampoule (h after the name). Negative angles have the top of the ampoules (flange side) rotated away from the source while the positive angles have the top rotated toward the source.

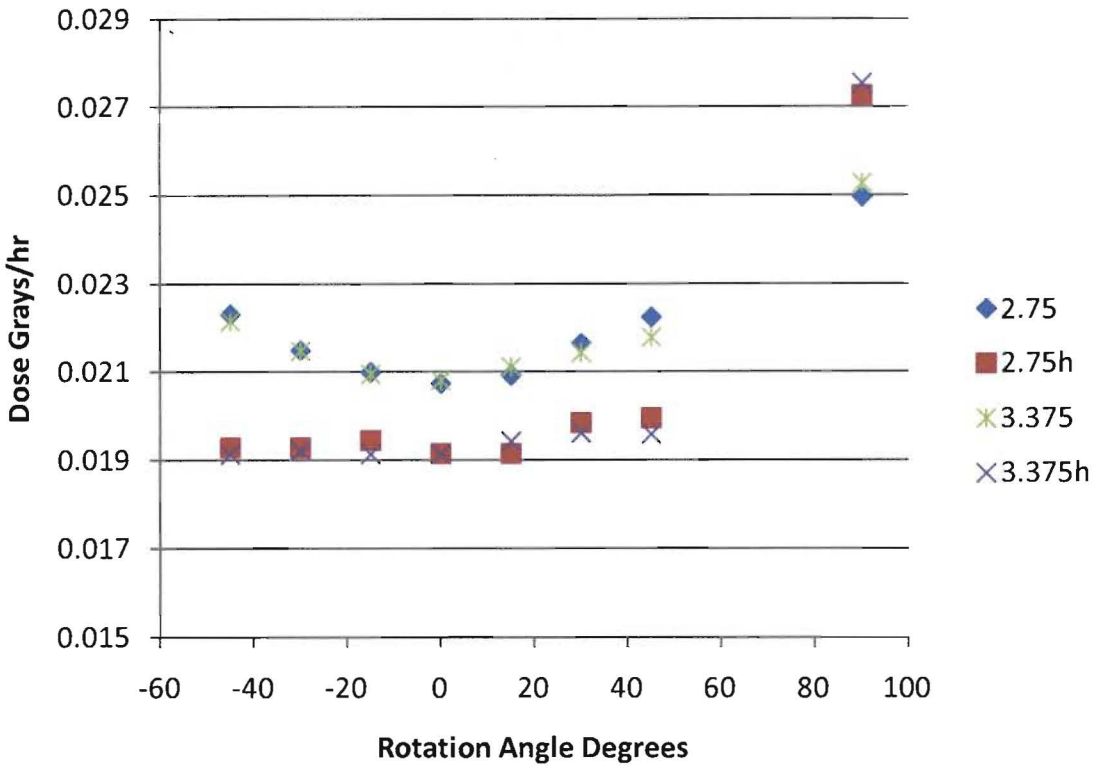

Figure 5. Dose rate as a function of ampoule angle w.r.t the source. The h after the name indicates results for ampoules covered by a heater coil. A positive angle is a rotation of the flange end toward the source, a negative angle is a rotation of the flange angle away from the source.

The tilting of the flange end of the ampoules increases the dose rate nearly the same regardless of whether the tilt is toward or away from the source. The uncovered ampoules are more sensitive to the smaller angle rotation than the heater ampoules, but less sensitive to the rotation of the ampoule to 90 degrees (the non-flange end is pointing toward the source). On average the heating coil ampoules receive about 10% less dose than the uncovered ampoules until they are rotated 90 degrees. The 90 degree rotation increases the dose rate by around 14% for ampoules without heaters and by 35% for ampoules with heaters. The small rotation ampoules have thinner amounts of LK3626 perpendicular to the source and more of the 662 keV photons penetrate through the ampoules and are not absorbed. The decreased sensitivity at the smaller angles for the heater ampoules must be due to the attenuation effects of the coils. At the 90 degree rotation, the on end orientation gives the 662 keV photons more LK3626 perpendicular to the source and more of the gammas are therefore absorbed. The heater coil ampoules absorb more gammas because the coils must behave as reflectors, helping to keep gammas scattering out of the LK3626 in the ampoules. This reflection is around an 8% effect on the 90 degree ampoules.

Similar simulations were performed with a ^{241}Am source. The dominant energy for the ^{241}Am are 59.5 keV gammas. These results are plotted in Figure 6 for both sets of ampoules with and without heater coils. The data sets are labeled with Am suffixes to indicate the ^{241}Am source.

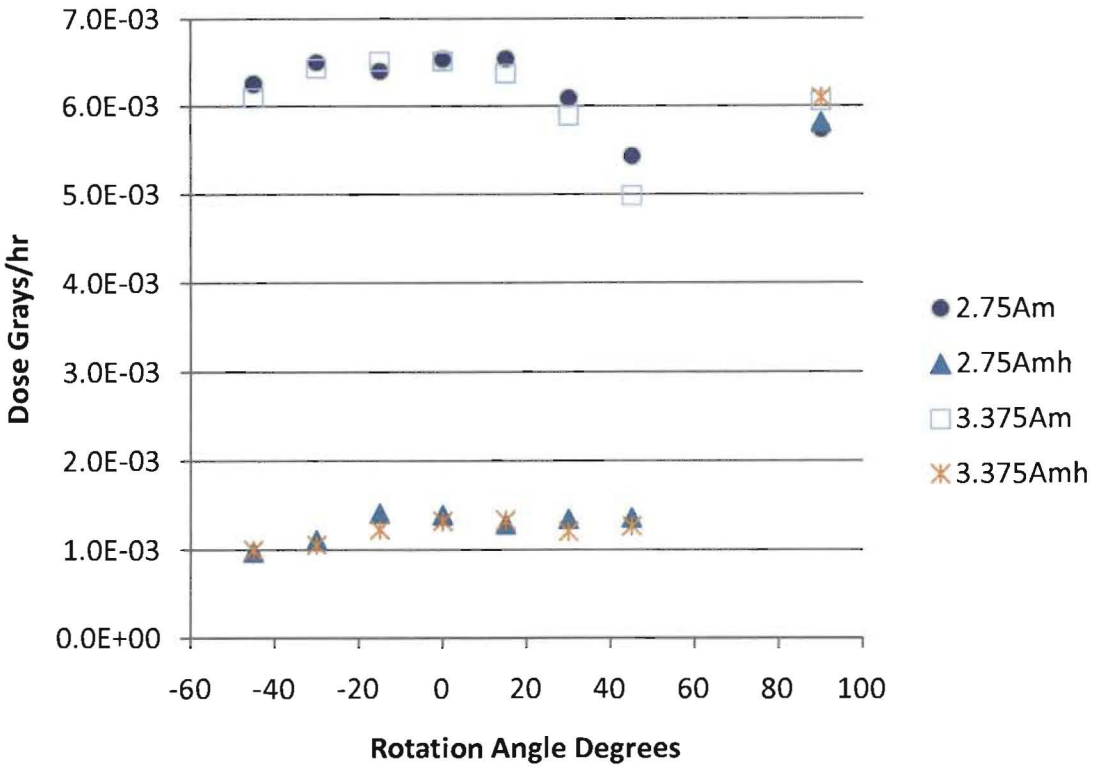

Figure 6. Dose rate as a function of ampoule angle w.r.t a ^{241}Am source. The h after the name indicates results for ampoules covered by a heater coil. A positive angle is a rotation of the flange end toward the source, a negative angle is a rotation of the flange angle away from the source.

The lower energy Am source provides a dose that is roughly 30% of the dose provided by the ^{137}Cs. The dose is even lower when the ampoule is surrounded by a coil, except in the 90 degree rotation case where the coil is not positioned between the source and the ampoule. The lower energy gammas from the ^{241}Am do not have the penetration power of the 662 keV gammas from the ^{137}Cs. Thus the ^{241}Am gammas do not penetrate through the ampoule and do not penetrate deep into the LK3626. The lower energy gammas do not have as much energy as the ^{137}Cs gammas and therefore cannot deposit as much energy when absorbed. The flanges and the heater coils also act as shielding to the lower energy gammas. The heater coils around the ampoules reduce the dose rate by nearly 80%. With a ^{241}Am source, ampoules without heater coils receive maximum dose when the ampoule is not rotated. The ampoules with heater coils receive the maximum dose when they are rotated 90 degrees. That orientation exposes the bottom of the ampoule to the source without any cover from the coil. Ampoules exposed to a ^{241}Am source will need more than three times the exposure time to match the dose from ^{137}Cs.

Dose contributions from scatter off the lead walls are shown in Figure 7. The scatter contributions are around two orders of magnitude or smaller than the total dose at 15cm from the source.

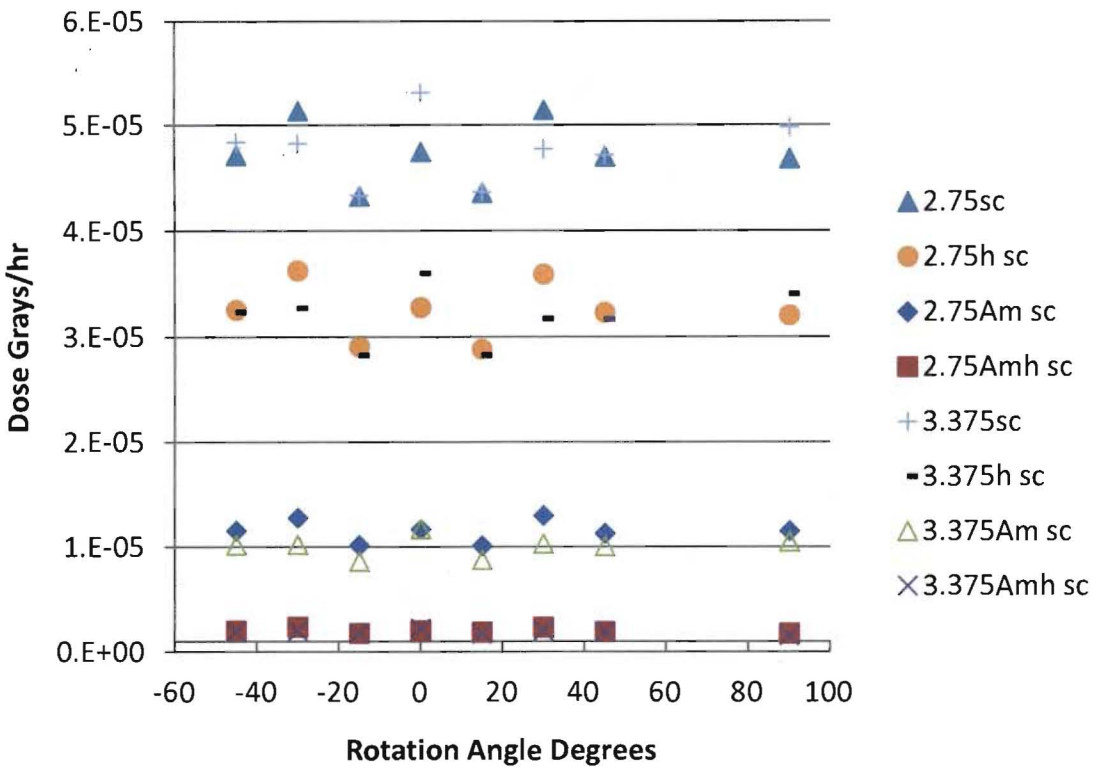

Figure 7. Dose rate from scatter as a function of ampoule angle w.r.t the source. The h after the name indicates results for ampoules covered by a heater coil. A positive angle is a rotation of the flange end toward the source, a negative angle is a rotation of the flange angle away from the source.

Scattered photons are less energetic than the gammas direct from the source. Thus the scattered photons are attenuated more by the heater the coil than direct gammas. The lower energy gammas from the ^{241}Am have scatter contributions which are 80% less than the ^{137}Cs scatter. Scattered photons enter the LK3626 from all directions while the direct gammas hit the LK3626 predominately from the direction of the source. Thus the ampoule rotation has little effect on the dose rate from scatter.

Dose rate calculations for different materials of interest were performed for both sets of ampoules. The ampoules were placed 23 cm from the source and were not rotated. The lists and compositions of materials are given in Tables 1 and 2. The tables are divided into two sets of materials. The first table consists of different polymers of interest. The second table consists of different binder materials for high explosives. The weight fraction compositions expressed in terms of the dominant elements are shown in the tables.

Table 1. Weight fraction compositions of polymers in the calculations.

Materials	LK3626	SX358	DC745	UNI620-3	M9787-C	VCE
wt %C	0.2780	0.2673	0.1937	0.2673	0.2673	0.1883
wt %H	0.0573	0.0599	0.0416	0.0599	0.0599	0.0260
wt %B	0	0	0	0	0	0.7141
wt %F	0	0	0	0	0	0
wt %Cl	0	0	0	0	0	0
wt %N	0.0196	0.0047	0	0.0047	0.0047	0
wt %O	0.2880	0.2838	0.3413	0.2838	0.2838	0.0717
wt %Al	0.0006	0	0	0	0	0
wt %Si	0.3467	0.3843	0.4234	0.3843	0.3843	0
wt %Sn	0.0098	0	0	0	0	0
Density (gm/CC)	0.546	0.4-0.8	1.35	1.27	1.16	1.77

Table 2. Weight fraction compositions of binders in the calculations.

Materials	KelF 800	Viton A	THV220G	Estane 5703	BDNPA/F (NP)	Est/NP Binder
wt %C	0.2324	0	0.2847	0.6200	0.2687	0.4446
wt %H	0.0049	0.3210	0.0104	0.0745	0.0391	0.0562
wt %F	0.5055	0.0189	0.7049	0	0	0
wt %Cl	0.2572	0.6601	0	0	0	0
wt %N	0	0	0	0.0235	0.1671	0.0955
wt %O	0	0	0	0.2820	0.5250	0.4037
Density (gm/CC)	2.02	1.85	1.95	1.19	1.39	1.28

The dose rates for the materials in both tables are shown in Figure 8. In Figure 9 the dose rates are normalized to the dose in LK3626, which is the baseline material used the radial and orientation dose rate calculations made previously.

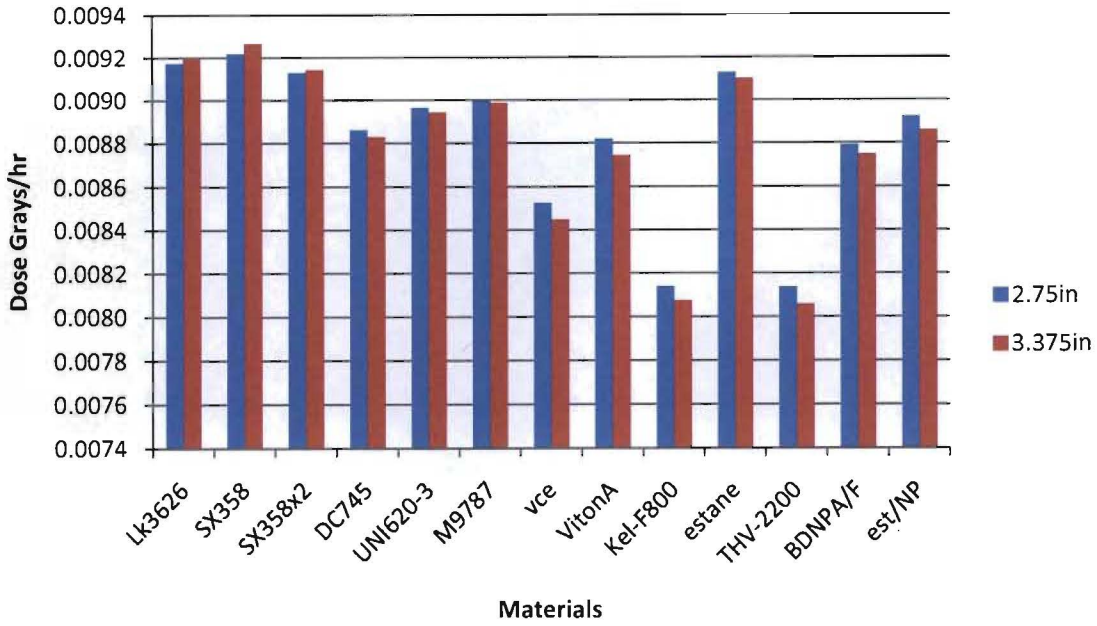

Figure 8. Dose rate plots for the different materials using 2.75in and 3.375in ampoules.

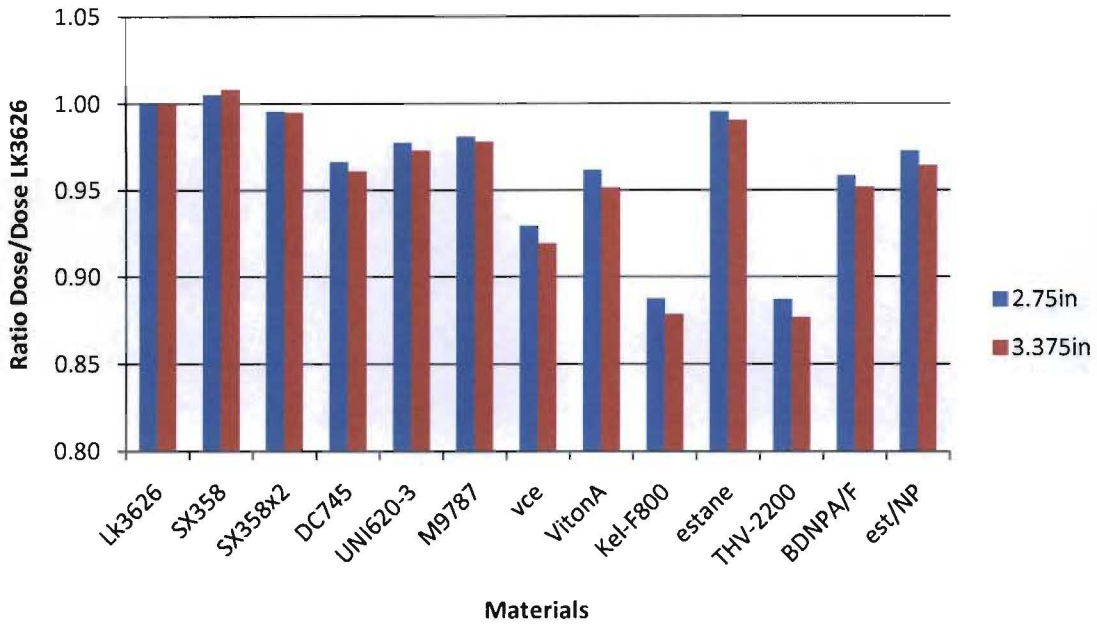

Figure 9. Plots of the dose in the different materials normalized by the dose in LK3626 for the 2.75in and the 3.375in ampoules.

The influence of the material density on the dose rate can be observed from the results for the SX358, SX358x2, UNI620-3, and M9787-C. The compositions of these materials are nearly identical (minus the trace elements) as seen in Table 1. Their densities range over 0.4 g/cc to 1.27 g/cc. The larger density further decreases the dose to the materials. The source of this effect may be increased backscattering from more dense materials. This

density/dose relationship appears to exist for all materials of different composition. The two lowest dose materials (Kel-F800 and THV-2200) have the highest densities and the two highest dose materials (SX358 and LK3626) have the lowest density. The relative dose to the materials appears to be inversely proportional to their relative density.

Summary

The empirical equations representing the dose rate to the ampoules as a function of distance from the ^{137}Cs source are given in the power law equations for the total curve in Figures 3 and 4. The ampoule dose rate has a $\sim 1/r^2$ dependency on the source distance. Scatter effects are less than a percent for a source centered in the cave and are a ~10% or less effect for a source in the corner of the cave.

Rotating the ampoules towards or away from the source increases the areal density of material exposed to the ^{137}Cs source. The larger areal density in the LK3626 captures more 662keVgammas from the ^{137}Cs and increases the dose rate absorbed in the LK3626. Similarly, the higher energy gammas from the ^{137}Cs have greater penetration through LK3626 when the ampoules are perpendicular to the source and have a smaller areal density. The increase in the areal density of the aluminum surrounding the LK3626 from rotation is insignificant to the dose absorbed in the LK3626. The higher energy of the ^{137}Cs gammas is not affected by the attenuation properties of the ampoule significantly. This rotation effect of the ampoules is reversed for the lower energy gammas (~60keV) from the ^{241}Am. The rotation decreases the dose rate to the ampoules since the rotation increases the areal density of the aluminum in the ampoules seen by the gammas coming from the source. The 60keV gammas from the ^{241}Am do not have the energy to "blast" through the ampoule walls as easily as the 662 keV ^{137}Cs gammas. In addition, the ^{241}Am gammas do not have as much energy per photon to dump into the LK3626 once they make it to the LK3626 in the ampoule. Therefore the dose rate to the ampoules is not increased when rotated and fewer gammas transmit through the LK3626 for the ^{241}Am source. Rotation of the ampoules has no effect on the amount scattered photons absorbed in the LK3626 for both sources. Scattered photons reach the ampoules from all angles. Thus rotating the ampoules does not affect the areal density seen by the scattered photons on average in the same way it affects gammas coming directly from the source.

The heating coils reduce the dose rate to the LK3626 by around 10-15% for the ^{137}Cs and by 17-20% for the ^{241}Am source. Once the gammas penetrate through the coils, the coils act as a reflector to help keep the gammas and their scatter products in the ampoule. This is evident from the flip in dose rate for ampoules with and without heating coils that are positioned on end (90 degrees to the source).

Finally, the simulations on the trade space materials show that the relative dose to all other materials appears to be inversely proportional to their relative density. The higher density materials have a smaller dose rate than the lower density materials. I have speculated that it is an increase in backscatter from the higher density materials that accounts for this property. Additional simulations could be performed to verify this by taking current tallies at the surface of the LK3626 and the ampoules.